Introducing Satellite Data Based Biosphere Model BEAMS to Improve Regional Transport Model for Estimating CO2 Emission from Mega-city Tokyo

Qiao Wang[1], Ryoichi Imasu[2], Satoshi Ito[1], Takahiro Sasai[3], and Hiroaki Kondo[4]

[1]Atmosphere and Ocean Research Institute The University of Tokyo
[2]Atmosphere and Ocean Research Institute University of Tokyo
[3]Tohoku University
[4]National Institute of Advanced Industrial Science and Technology (AIST)

November 23, 2022

Abstract

GOSAT (Greenhouse gases Observing SATellite) observations ameliorate inversion analysis of greenhouse gas emissions. Mesoscale atmospheric transport model (AIST-MM, National Institute of Advanced Industrial Science and Technology-Mesoscale Model) and global-scale transport model (NICAM-TM, Nonhydrostatic ICosahedral Atmospheric Model-Transport Model) have been coupled for GOSAT data assimilation in order to estimate CO2 emission from mega-city Tokyo. However, forests in the north and west of Kanto region, of which Tokyo Metropolis is the center, generate significant biogenic CO2 fluxes and such atmosphere-biosphere gas exchange remains to be properly calculated during the modeling processes. In this study, we use MODIS products to simulate regional GPP (gross primary production), vegetational and soil respirations based on BEAMS (Biosphere model integrating Eco-physiological And Mechanistic approaches using Satellite data) algorithms. By integrating this atmosphere-terrestrial ecosystem carbon balance module to our regional inversion analysis, we aim at more precise estimation of CO2 emission from Tokyo. Reference https://doi.org/10.1175/1520-0450(1995)034<1439:TTILWA>2.0.CO;2 https://doi.org/10.2151/jmsj.79.11 https://doi.org/10.2151/jmsj.2011-306 https://doi.org/10.1029/2005JG000045 https://doi.org/10.1016/j.rse.20

AGU Fall Meeting 2018 | Washington DC. | **A43R-3446**

Introducing Satellite Data Based Biosphere Model BEAMS to Improve Regional Transport Model for Estimating CO_2 Emission from Mega-city Tokyo

Qiao Wang[1)] (qwang@aori.u-tokyo.ac.jp), **Ryoichi Imasu**[1)]
Satoshi Ito[1)], **Takahiro Sasai**[2)], **Hiroaki Kondo**[3)]

1) Atmosphere and Ocean Research Institute (AORI), The University of Tokyo, 5-1-5 Kashiwanoha, Kashiwa-shi, Chiba 277-8568, Japan; 2) Department of Geophysics, Graduate School of Science, Tohoku University, 6-3, Aramaki Aza-Aoba, Aoba-ku, Sendai 980-8578, Japan; 3) National Institute of Advanced Industrial Science and Technology (AIST), 16-1 Onogawa, Tsukuba, Ibaraki 305-8569, Japan

I. Introduction

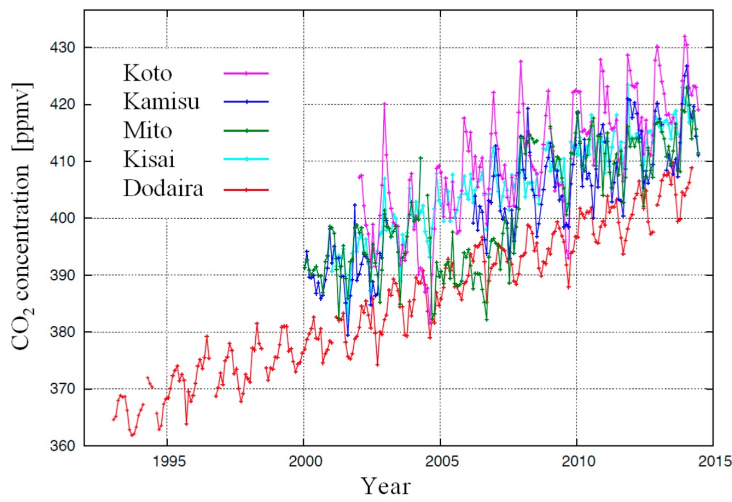

Figure 1. Monthly mean CO_2 concentrations observed at five sites in and around Tokyo from 1992 to 2015, showing obvious seasonal CO_2 concentration variations Imasu and Tanabe, 2018

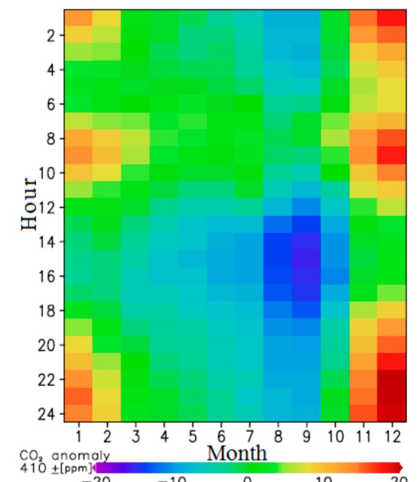

Figure 2. Diurnal–monthly anomalies of CO_2 concentrations in Koto, Tokyo (35°40'N, 139°49'E), showing lowest CO_2 level in summer afternoon and highest at winter night, Imasu and Tanabe, 2018

In summer, forests west and north of Tokyo Metropolis in the Kantō plain cause significant CO_2 fluxes. These land-atmosphere CO_2 exchanges, however, have yet to be realistically simulated in the regional transport model AIST-MM (AIST-Mesoscale Model, Kondo *et al.*, 2001). With the objective of estimating Tokyo's CO_2 emission inventory using a top-down approach, this study plans to improve regional CO_2 concentration simulation accuracy by

- integrating BEAMS (Biosphere model integrating Eco-physiological And Mechanistic approaches using Satellite data, Sasai *et al.*, 2005; 2011) photosynthesis and respiration components to the numerical simulation
- introducing GOSAT (Greenhouse gases Observing SATellite) data to the AIST-MM based inverse model

We expect the updated model to better simulate both seasonal and diurnal CO_2 variations in the region, which Imasu and Tanabe 2018 (Fig. 1 and 2) have observed in ground CO_2 observational concentrations analysis.

II. Simulations

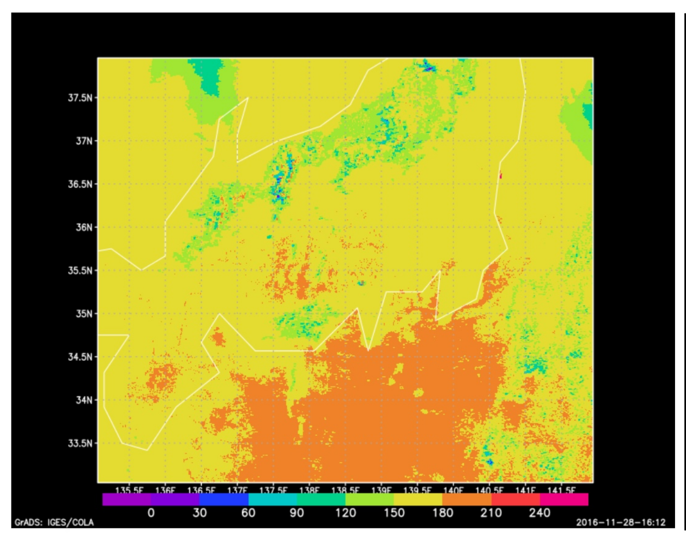

Figure 3. JASMES Photosynthetically Active Radiation (PAR, Frouin *et al.*, 2007)

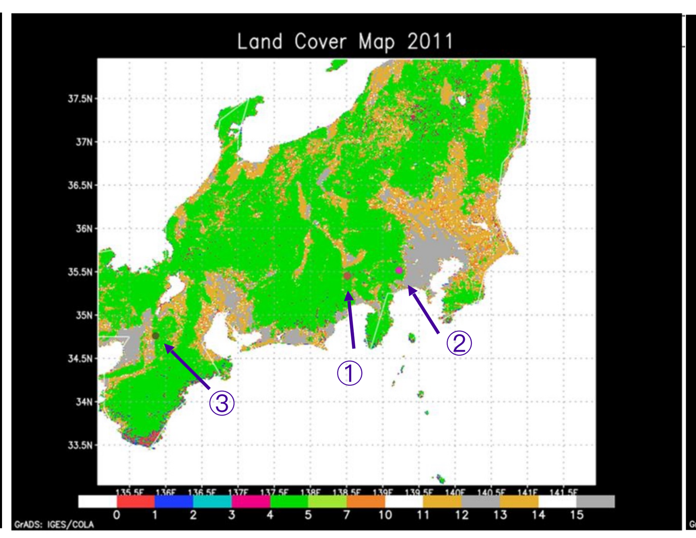

Figure 4. MODIS Land Cover Type (MCD12Q1, Friedl *et al.*, 2010)

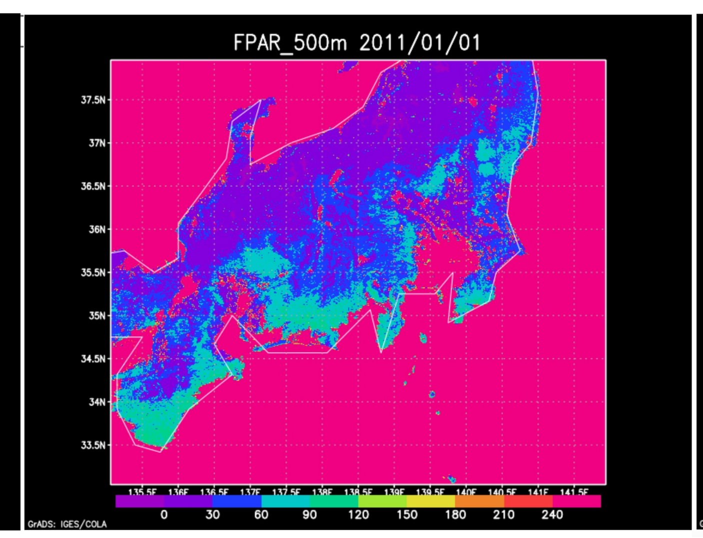

Figure 5. MODIS Faction of absorbed PAR (FPAR, MCD15A3H, Myneni *et al.*, 2015)

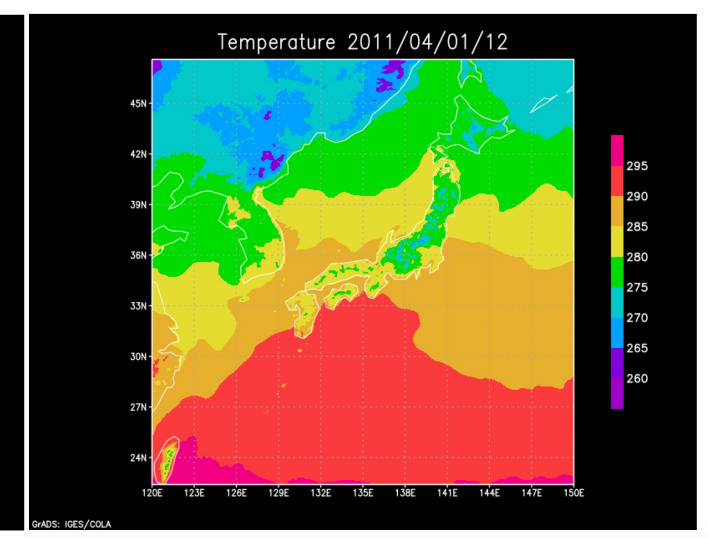

Figure 6. GPV-JMA (Grid Point Values-Meso Scale Model) ground temperature

Recalibrating JASMES PAR data by comparison with ground observational PAR in Tsukuba, Japan

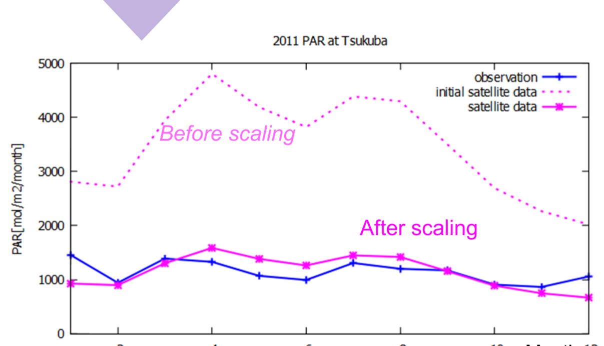

Figure 7. JASMES PAR data before and after scaling

Scaling factor 0.33036

$$GPP = APAR \times LUE$$
$$APAR = PAR \times FPAR$$
$$LUE = LUE_{max} \times Stress$$
$$Stress = P_{actual} / P_{max}$$
$$P = \min \{P_l, P_s, P_m\}$$

$$P_m = 0.5 \times V_{cmax}$$
$$P_s = (V_{cmax} \times (p_i - \Gamma^*)/(p_i + K_c \times (1 + O_2/K_o))$$
$$P_l = (J \times (p_i - \Gamma^*)/(4 \times (p_i + 2 \times \Gamma^*))$$
$$K_c = K_{c25} \times Q_{10Kc}{}^{(temp - 298.5)/10}$$
$$K_o = K_{o25} \times Q_{10Ko}{}^{(temp - 298.5)/10}$$
$$V_{cmax} = V_{cmax25} \times Q_{10Vcmax}{}^{(temp - 298.5)/10} \times F_{soil1}$$
$$F_{soil1} = 1/(1 + \exp(0.02 \times (\Psi - \Psi_{wp})))$$
$$F_{soil2} = (\Psi - \Psi_{wp})/(\Psi_{fc} - \Psi_{wp})$$

$$\Psi = \Psi_s \times V^{-B}$$
$$\Gamma^* = (P\_atm \times O_{xy})/(2 \times \tau)$$
$$\tau = \tau_{25} \times Q_{10tau}{}^{(temp - 298.5)/10}$$
$$\theta_j \times J^2 + (J_{max} + I_j) \times J + J_{max} \times I_j = 0$$
$$P_n = P - R_d = G \times (p_{atm} - p_i)/P\_atm$$
$$1/G = 1/G_{st} + 1/G_{bl}$$
$$G_{st} = 1/1.6 \times (b + (m \times hs \times P_n)/(p_{atm} - \Gamma) \times F_{soil2})$$

Autotrophic Respiration

$$Ram_{leaf/stem/root} = kr_{leaf/stem/root} \times Cbio_{leaf/stem/root} \times Q10_{function}$$
$$Rag_{leaf/stem/root} = frg \times (GPP_{leaf/stem/root} - Ram_{leaf/stem/root})$$

Gross Primary Production (GPP) → **Net Primary Production (NPP)** → **Net Ecosystem Production (NEP)**

Heterotrophic Respiration

$$LF_{stem/root} = kl_{stem/root} \times Cbio_{stem/root}$$
$$LF_{leaf} = NPP_{leaf} - (Cbio_{leaf}(t) - (Cbio_{leaf}(t-1))$$
$$C_{flowi} = k_i \times L_c \times Cs_i \times D_{tw} \times (1 - M_i); i = 1,2$$
$$C_{flowi} = k_i \times T_m \times Cs_i \times D_{tw} \times (1 - M_i); i = 3$$
$$C_{flowi} = k_i \times Cs_i \times D_{tw} \times (1 - M_i); i = 4, 5, 6, 7, 8$$

1: surface structural C
2: root structural C
3: soil microbe
4: surface microbe
5: surface metabolic C
6: root metabolic C
7: slow C
8: passive C
9: leached C

Figure 8. BEAMS based algorithm (Sasai *et al.*, 2005; 2011), with GPP represents to the total carbon absorbed by photosynthesis, NPP represents to the total carbon captured by plants and NEP represents to the total carbon exchange between the ecosystem and atmosphere

APAR	absorbed PAR
LUE	light use efficiency
P	actual photosynthesis rate
P_l	light-limited rate of photosynthesis
P_s	ribulose-biophosphate carboxylase oxygenase limited rate
P_m	capacity for export or utilization of photosynthetic products
V_{cmax}	maximum rate of carboxylation
p_i	intercellular CO_2 pressure
Γ	compensation point
K_c	Michaelis-Menten constants for CO_2
K_{c25}	Michaelis-Menten constants for CO_2 at 25°C
temp	temperature
K_o	Michaelis-Menten constants for O_2
K_{o25}	Michaelis-Menten constants for O_2 at 25°C
J	rate of electron transport
Q_{10Kc}	Q10 value of Kc (=2.1)
Q_{10Ko}	Q10 value of Ko (=1.2)
$Q_{10Vcmax}$	Q10 value of Vcmax (=2.4)
Γ^*	CO_2 compensation point in the absence of dark respiration
F_{soil1}	stress value for Vcmax (range; 0.0 – 1.0)
Ψ	metric water potential
Ψ_{wp}	metric water potential at wilting point
F_{soil2}	soil water stress for stomatal conductance
Ψ_{fc}	water potential at field capacity
Ψ_s	metric water potential at saturation
V	volumetric soil moisture
B	slope of the retention curve on a logarithmic graph
P_n	leaf net assimilation rate
P_atm	atmospheric pressure
O_{xy}	O_2 concentration
τ	CO_2/O_2 specificity ratio
τ_{25}	CO_2/O_2 specificity ratio at 25°C
hs	relative air humidity
θ_j	curvature of leaf response of electron transport to irradiance (=0.7)
J_{max}	potential rate of electron transport
I_j	PAR effectively absorbed by PSII
R_d	dark respiration
G	total conductance to CO_2
p_{atm}	atmospheric CO_2 pressure
G_{st}	stomatal conductance
G_{bl}	boundary layer conductance
b	constant value 0.01
m	constant value 9.2
$Ram_{leaf/stem/root}$	autotrophic maintenance respiration (leave, stem, and root)
$Rag_{leaf/stem/root}$	autotrophic growth respiration (leave, stem, and root)
$kr_{leaf/stem/root}$	specific respiration rate (leave, stem, and root)
$Cbio_{leaf/stem/root}$	carbon content of biomass (leave, stem, and root)
$Q10_{function}$	temperature dependence of maintenance respiration (2.0)
frg	a fraction of growth respiration in the potential NPP (0.25)
$LF_{stem/root}$	litter fall (stem and root)
$kl_{stem/root}$	specific litter fall rate (stem and root)
LF_{leaf}	litter fall (leaf)
C_{flowi}	carbon fluxes
k_i	dark respiration
L_c	maximum decay rate constant of each soil carbon pool
Cs_i	effect of lignin content of structural material on structural decomposition
	carbon content of litter or SOM pool
D_{tw}	combined effect of soil water content and temperature on decomposition scalars (0.0–1.0)
TM	effect of silt plus clay content on active SOM turnover
M_i	carbon assimilation efficiency of soil microbes

References

Friedl M. et al., *Remo. Sens. Env.*, 114, 168-182, 2010, doi:10.1016/j.rse.2009.08.016

Imasu R, Tanabe Y. *Atmos.*, 9, 367, 2018, doi : 10.3390/atmos9100367

Kalnay E. et al., *Bull. Amer. Meteor. Soc.*, 77, 437-470, 1996, doi: 10.1175/1520-0477(1996)077<0437:TNYRP>2.0.CO;2

Kondo H. et al., *J. Meteor. Soc. Japan*, 79, 11-21, 2001, doi:10.2151/jmsj.79.11, 2001.

Myneni R. et al., *MCD15A3H*, doi: 10.5067/MODIS/MCD15A3H.006

Niwa Y. et al., *J. Meteor. Soc. Japan*, 89, 255-268, doi:10.2151/jmsj.2011-306, 2011.

Sasai T. et al., *J. Geophys. Res.*, 110, doi: 10.1029/2005JG000045, 2005.

Sasai T. et al., *Remo. Sens. Env.*, 115, 1758-1771, 2011.

* http://www2.ffpri.affrc.go.jp/labs/flux/

III. Preliminary results

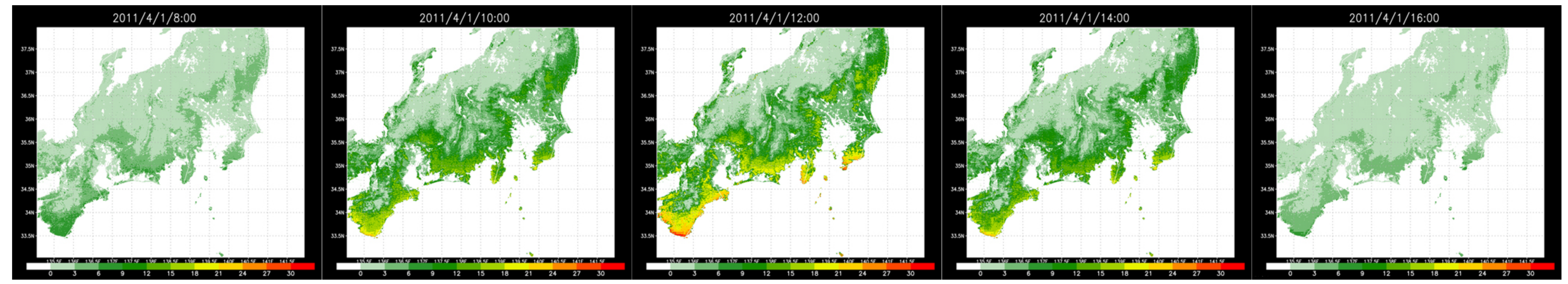

Figure 9. An set of examples of photosynthesis (GPP, $gC/m^2/hour$) diurnal variations at 8:00, 10:00, 12:00, 14:00 and 16:00, April 1st 2014

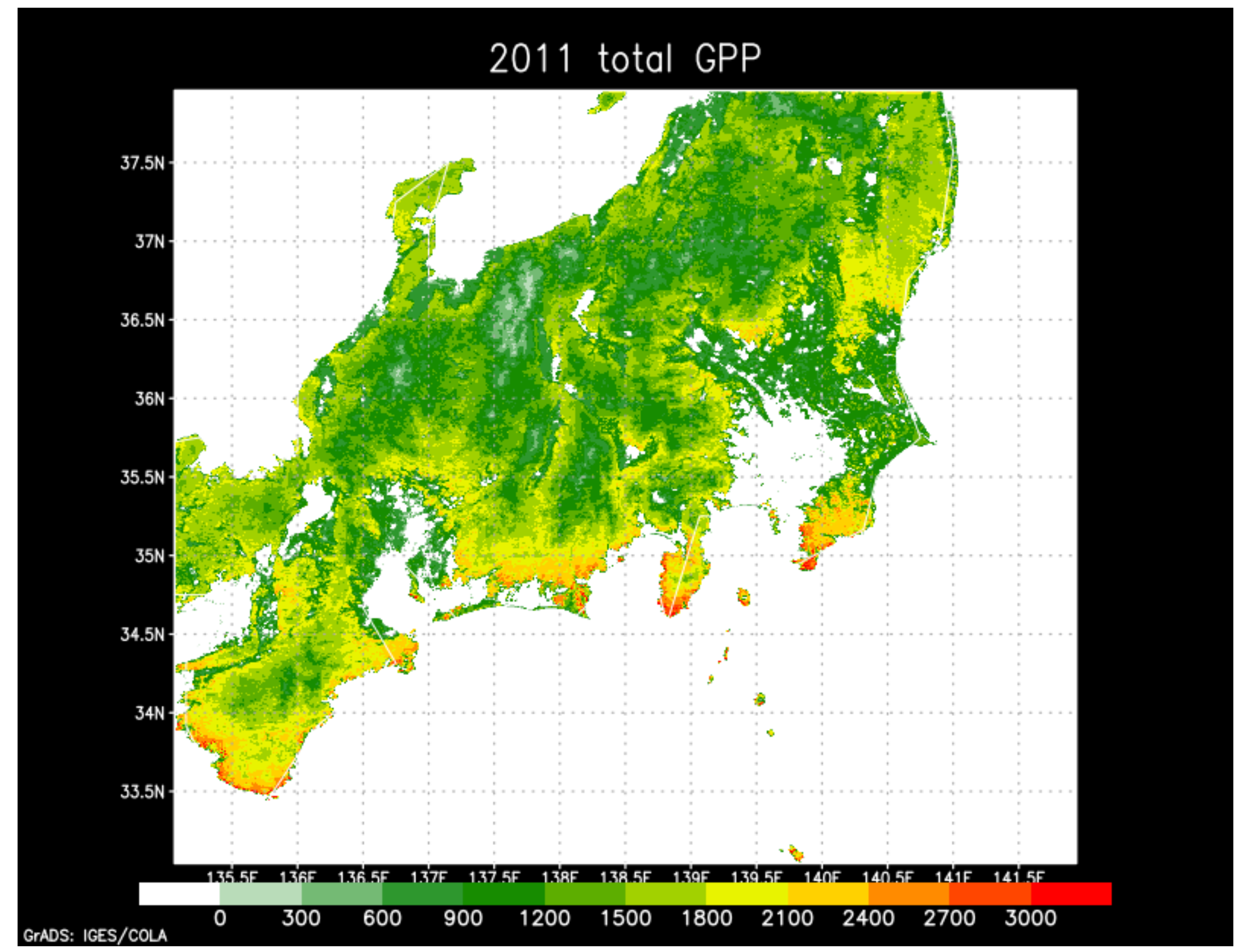

Figure 10. Total carbon absorbed by photosynthesis (GPP, $gC/m^2/year$) in 2011

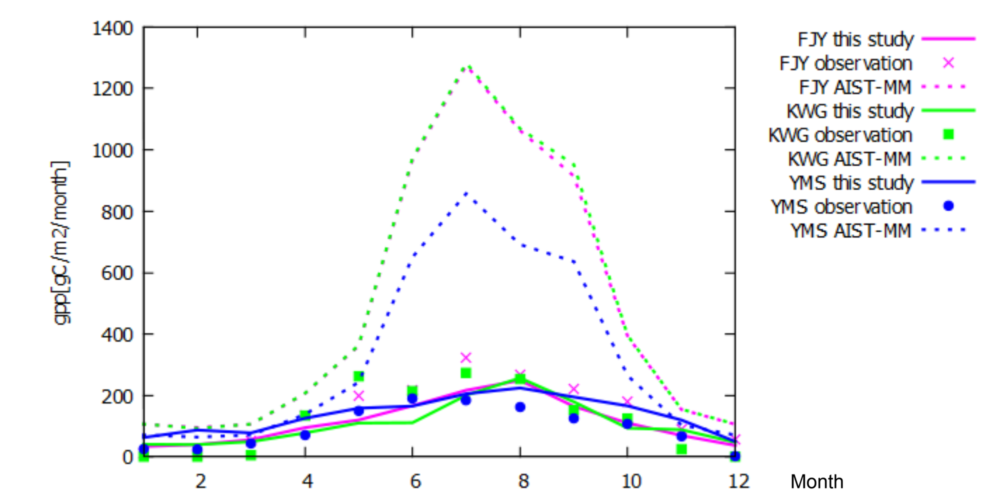

Figure 11. Simulated GPP by BEAMS-GPP (—), simulated GPP by pre-optimized AIST-MM (- -) and GPP data from three observational sites in Japan over 2011

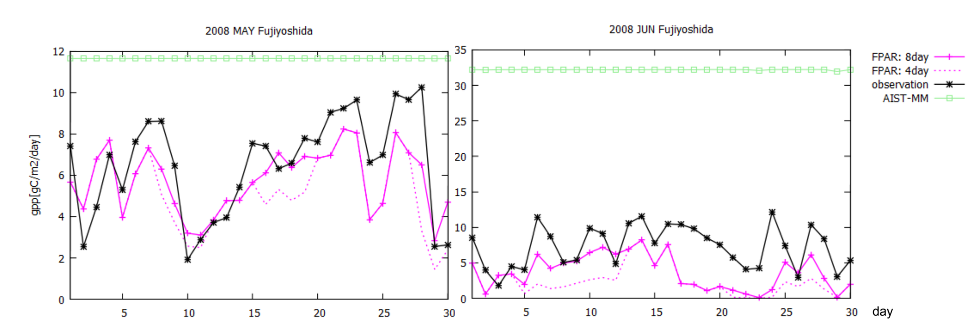

Figure 12. Comparison of BEAMS-GPP using 8-day MODIS FPAR or 4-day MODIS PAR with pre-optimized AIST-MM GPP and GPP data in Fujiyoshida, 2011 summer

Table 1. Information about three Japanese Forestry and Forest Products Research Institute (FFPRI) FluxNet sites* for calculated GPP validation (locations in Fig. 4)

Site name	Abbreviation	Latitude	Longitude	Year	Forest type
Fujiyoshida	① FJY	35°27'N	138°46'E	2008	evergreen coniferous
Kawagoe	② KWG	35°52'N	139°29'E	2002	deciduous broadleaf
Yamashiro	③ YMS	34°48'N	135°51'E	2005	mixed

IV. Future work

- Introduce respiration (plant, soil) components to the model
- Validate the simulation results of net carbon exchange between the forests and atmosphere with ground observations
- Apply GOSAT CO_2 data to the inverse modeling of CO_2 emissions from mega-city Tokyo
- Compare inverse modeling results with bottom-up inventories (i.e. ODIAC, EDGAR)
- Future application of optimized AIST-MM to update regional CO_2 emission inventory

Table 2. Potential finer input data list for future simulations

Atmospheric transport part	BEAMS part
GPV-MSM data	MODIS Land Cover Type (MCD12Q1, Friedl *et al.*, 2010)
	GCOM-C (Global Change Observation Mission - Climate) or JASMES PAR**
GOSAT CO_2 concentrations	**GCOM-C** or MODIS LAI and fPAR**
Emission inventory provided by the Ministry of Environment of Japan**	Air temperature, precipitation, vapor pressure (GPV-JMA)
	GCOM-C above ground biomass (AGB)**
	SMAP (Soil Moisture Active Passive mission) soil moisture*

** To be decided depending on the year and availability of data